



Open Archive TOULOUSE Archive Ouverte (OATAO)

OATAO is an open access repository that collects the work of Toulouse researchers and makes it freely available over the web where possible.

This is an author-deposited version published in : <http://oatao.univ-toulouse.fr/Eprints> ID : 4707

To link to this article : DOI : [10.1016/j.polymer.2010.07.040](https://doi.org/10.1016/j.polymer.2010.07.040)

URL : <http://dx.doi.org/10.1016/j.polymer.2010.07.040>

To cite this version : Capsal, Jean-Fabien and Dantras, Eric and Dandurand, Jany and Lacabanne, Colette (2010) *Dielectric relaxations and ferroelectric behaviour of even-odd polyamide PA 6,9*. Polymer, vol. 51 (n° 20). pp. 4606-4610. ISSN 0032-3861

Any correspondence concerning this service should be sent to the repository administrator: staff-oatao@inp-toulouse.fr.

Dielectric relaxations and ferroelectric behaviour of even–odd polyamide PA 6,9

Jean-Fabien Capsal, Eric Dantras*, Jany Dandurand, Colette Lacabanne

Laboratoire de Physique des Polymères, Institut CARNOT-CIRIMAT, Université Paul Sabatier, 31062 Toulouse cedex 09, France

A B S T R A C T

Thermo Stimulated Current (TSC) combined with Dynamic Dielectric Spectroscopy (DDS) have been applied to the investigation of dielectric relaxation modes of an even–odd Polyamide PA 6,9. The correlation between results obtained by both methods allows us to describe precisely the molecular mobility. At high temperature, the various dielectric relaxation phenomena are separated by applying the dielectric modulus formalism. The comparison between the activation enthalpy values obtained by DDS and TSC leads to the assignment of the so-called α mode to cooperative movements of polymeric sequences. Molecular mobility of PA 6,9 is compared with the one of PA 11. The piezoelectric activity of PA 6,9 is shown and analyzed.

Keywords:
Dielectric
Relaxations
Piezoelectric

1. Introduction

Piezoelectric polymers have been the subject of a lot of work since the discovery of the piezoelectric behaviour of poly(vinylidene fluoride) PVDF by Kawai in 1969 [1]. The understanding of the molecular origin of the ferroelectricity of PVDF [2–4] initiates the development of its vinylidene fluoride–trifluoroethylene copolymers [5,6] (P(VDF-TrFE)) and vinylidene fluoride–trifluoroethylene–chlorofluoroethylene terpolymers [7,8] (P(VDF-TrFE-CFE)). Scheinbeim et al. [9], discovered the ferroelectric behaviour of odd numbered polyamides and showed that the remanent polarization is linearly dependent upon the dipolar density of amide groups. More recently, a new class of even–odd polyamide PA 6,9 has been elaborated. Franco et al. [10], demonstrate that the room temperature crystalline structure of PA 6,9 differs from the classic hydrogen bonded sheet structure of PA 6,6. From a structural point of view, PA 6,9 might have analogies with odd-even polyamides but the corresponding studies are mostly concentrated on the crystalline structures and mechanical properties [11]. As far as we know, the dielectric and the ferroelectric behaviour of even–odd polyamides have not yet been shown. In this work, molecular mobility of dipolar entities of polyamide 6,9 has been characterized using a combination of thermo stimulated current (TSC) and dynamic dielectric spectroscopy (DDS). For the first time, polarization and piezo/pyroelectric coefficients have been measured showing the ferroelectric behaviour of polyamide 6, 9.

2. Experimental section

2.1. Dielectric analyses

The polyamide 6,9 films were elaborated by melting the polymer powder at 240 °C in a hot press. The crystallinity ration χ_c of PA 6,9 obtained by DSC was measured near 16%. DDS was performed on unstretched films of about 100 μm . In this case, a humidity content of 1% has been determined by thermogravimetry analyses [12]. A Novocontrol Broadband Dielectric Spectrometer system BDS 400 was used to measure the dielectric permittivity on extended temperature and frequency scales. Isothermal measurements were carried out in the frequency range of 10^{-1} to 10^6 Hz for temperature varying from -150 to 150 °C by steps of 5 °C. The complex dielectric permittivity ε^* extracted from dynamic dielectric spectroscopy (DDS) was recorded as a function of angular frequency ω and fitted by the Havriliak–Negami function [13]:

$$\varepsilon^*(\omega) = \varepsilon_\infty + \frac{(\varepsilon_s - \varepsilon_\infty)}{(1 + (i\omega\tau)^{\beta_{\text{HN}}})^{\gamma_{\text{HN}}}} \quad (1)$$

where ε_s is the static permittivity, ε_∞ is the permittivity at high frequency, and β_{HN} , γ_{HN} are the Havriliak–Negami parameters. But for symmetric mode (Cole Cole) as β relaxation for example, the γ_{HN} parameter is equal to 1.

The dielectric loss modulus M'' is deduced from the real and the imaginary part of the dielectric permittivity ε' and ε'' , according with the relationship:

* Corresponding author.
E-mail address: dantras@cict.fr (E. Dantras).

$$M'' = \varepsilon'' / (\varepsilon'^2 + \varepsilon''^2) \quad (2)$$

In the modulus formalism, Maxwell–Wagner–Sillars (MWS) polarization which usually occurs in heterogeneous systems like semi-crystalline polymers [14,15] is observed as a mode. In the ε'' formalism, the MWS peak is sometimes hidden by the conductivity rise.

TSC analyses were carried out on a TSC/RMA analyser. For recording complex thermograms, the sample was polarized by an electrostatic field $E_p = 1 \text{ MV.m}^{-1}$ during $t_p = 2 \text{ min}$ over a temperature range from the polarization temperature $T_p = 90 \text{ }^\circ\text{C}$ down to the freezing temperature $T_0 = -160 \text{ }^\circ\text{C}$. Then the field was turned off and the depolarization current was recorded with a constant heating rate ($q_h = + 7 \text{ }^\circ\text{C.min}^{-1}$), the equivalent frequency of the TSC spectrum was $f_{eq} \sim 10^{-2} - 10^{-3} \text{ Hz}$. Elementary TSC thermograms were recorded with a poling window of $5 \text{ }^\circ\text{C}$. Then the field was removed and the sample cooled down to a temperature $T_{cc} = T_p - 30 \text{ }^\circ\text{C}$. The depolarization current was recorded with a constant heating rate q_h . The series of elementary thermograms was recorded by shifting the poling window by $5 \text{ }^\circ\text{C}$ towards higher temperature.

2.2. Ferroelectric analyses

For ferroelectric measurements, films were cold-drawn at room temperature. In order to prevent voltage breakdown during the poling procedure, the samples were covered by Castor oil and measurements were made at low pressure ($p = 2 \times 10^{-4} \text{ hPa}$). The samples were poled under triangular shape electric field at room temperature.

Piezoelectric measurements were carried out using a PM 200 piezometer supplied by Piezotest, with a strength of 0.25 N at 110 Hz in frequency. The piezoelectric coefficient d_{33} is measured in the same direction than the polarization field.

Pyroelectric measurements were performed by a Keithley femto-amperemeter. The samples were short-circuited during 5 min at room temperature and cooled to $-170 \text{ }^\circ\text{C}$. They were heated up to $100 \text{ }^\circ\text{C}$ with a constant heating rate q_h to eliminate thermally stimulated currents. Then, they were cooled again to $-170 \text{ }^\circ\text{C}$ and the pyrocurrent was recorded as a function of temperature. The pyroelectric coefficient p is proportional to the heating rate and to the sample surface as indicated by its definition:

$$p = \frac{i(T)}{q_h \times S} \quad (3)$$

where $i(T)$ is the current (A) as a function of temperature, S is the surface area (m^2). Piezoelectric measurements were carried out after the pyroelectric tests to prevent any spontaneous poling effect (internal stresses).

3. Results and discussion

3.1. Dielectric relaxation

3.1.1. Isothermal dielectric response

The molecular dynamics of the dipolar entities of PA 6,9 in the high frequency range has been analyzed by dynamic dielectric spectroscopy. The dielectric modulus losses M'' are presented in Fig. 1. This formalism allows a better resolution of high temperature modes that could be partially hidden by the MWS contribution.

Six relaxation modes are pointed out on the 3D dielectric relaxation map. The low temperature γ mode is attributed to the

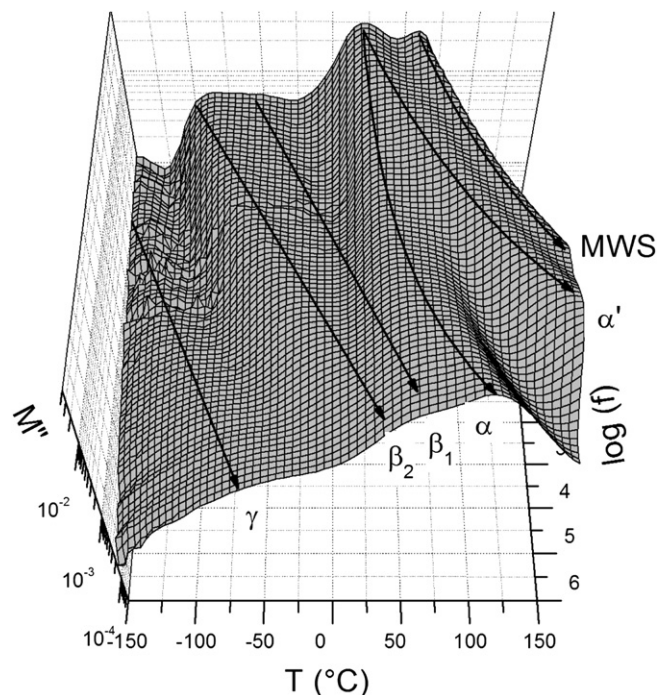


Fig. 1. 3D relaxation map of the dielectric modulus losses of PA 6,9 from DDS.

molecular mobility of aliphatic sequences of PA 6,9. It is now generally accepted in polyamides that the γ relaxation involves a mobility of the methylene groups between amide linkages [16]. The β_2 and β_1 sub-modes are related to the mobility of water–amide complexes and free amide groups respectively [17]. The α and α' relaxations are attributed to the dielectric manifestation of glass transition in the free amorphous phase and the amorphous phase constrained by the crystallites respectively [18]. The MWS mode is associated with heterogeneities induced by crystalline/amorphous interfaces [19].

3.1.2. Thermo stimulated dielectric response

The dynamic of dipolar entities of polyamide 6,9 in the low frequency range has been studied using the TSC technique. The complex TSC thermogram is reported in Fig. 2. Four relaxation

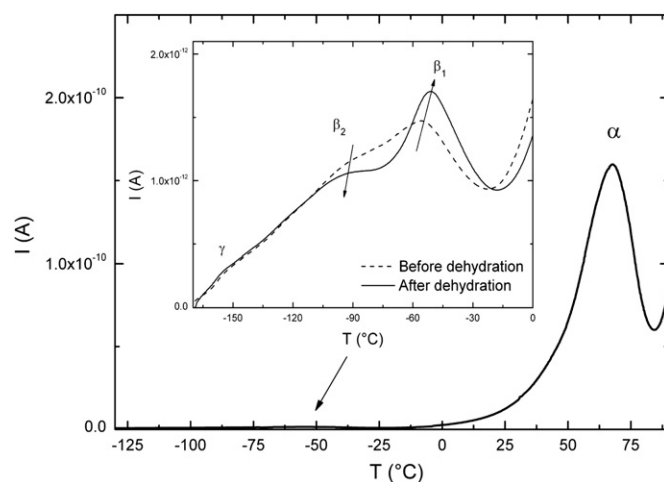


Fig. 2. Global TSC thermogram of PA 6,9 ($E = 1 \text{ MV/m}$, $T_p = 90 \text{ }^\circ\text{C}$). In the insert, low temperature relaxations before (1) and after (2) dehydration are shown.

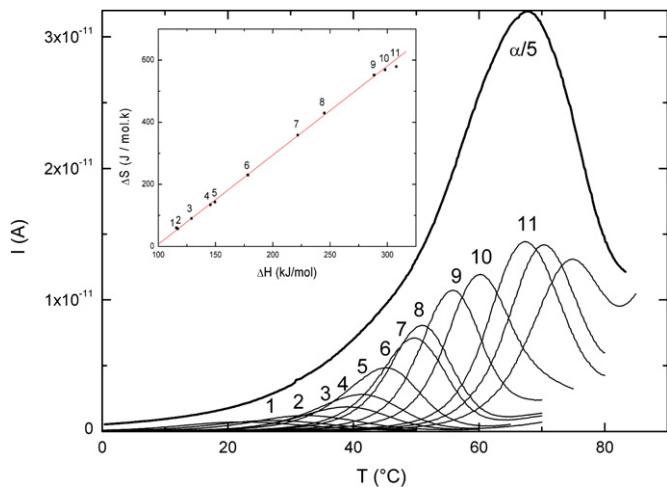


Fig. 3. Fractional and global (amplitude divided by 5) TSC thermograms of PA 6,9 for α mode. In the insert the activation entropy versus the activation enthalpy of each elementary process are reported.

modes are pointed out. The low temperature γ relaxation at -150°C has been attributed to the molecular mobility of aliphatic sequences of polyamide 6,9. The β relaxations involve the amide groups of macromolecules. In order to establish the molecular origin of the two components of this mode (β_1 and β_2), the sample was dehydrated at 120°C for 30 min. The insert of Fig. 2 represents the TSC thermograms of PA 6,9 before (dashed line) and after (solid line) dehydration, respectively. Amide groups are known to interact with water molecules. For a dehydrated sample, the amplitude of the β_2 mode decreases and the one of β_1 increases. Moreover, we note an anti plasticization phenomenon for the β_1 mode. These evolutions of β modes allow us to attribute the β_1 component to free amide groups and the β_2 component to the water–amide complex relaxation [11]. The main dipolar relaxation called α mode is located at $T_\alpha = 70^\circ\text{C}$. This relaxation occurs in the temperature range of the polyamide 6,9 glass transition T_g as already observed by differential scanning calorimetry [12]. Indeed all α and β relaxations are associated with polar amide groups, the large relaxation magnitude of the α mode regarding the β one is due to the delocalisation of the molecular mobility along the main chain over a sequence of several nanometers. Contrarily the β mode only implies oscillation of the amide group or amide–water complex.

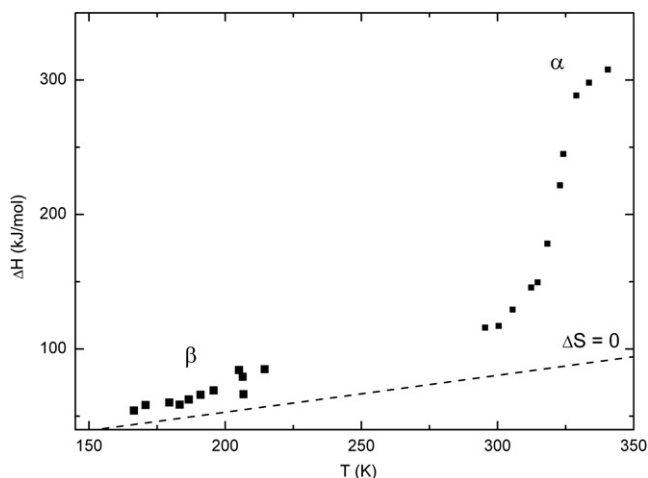


Fig. 4. Activation enthalpy versus temperature extracted from TSC elementary processes for β and α relaxation modes of PA 6,9.

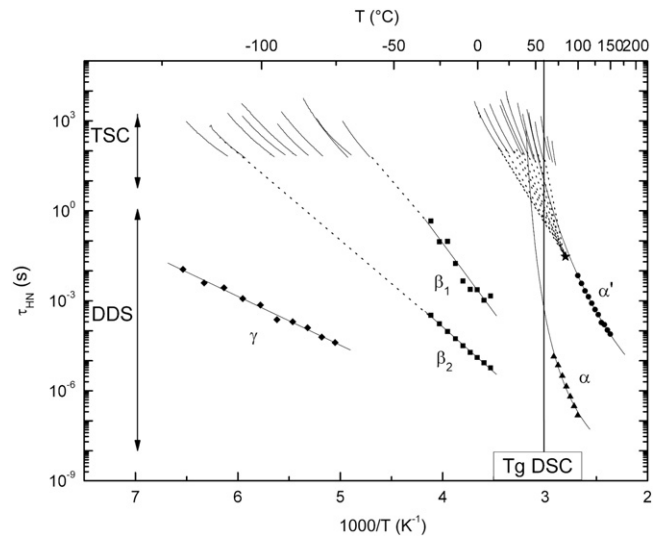


Fig. 5. Arrhenius diagram of the relaxation modes of PA 6,9 from combined DDS and TSC.

Fig. 3 shows the fractional TSC thermograms of the α mode of PA 6,9. From the elementary processes, activation enthalpy (ΔH) and pre-exponential factor (τ_0) has been extracted. Activation entropy ΔS has been calculated from τ_0 values. The values of ΔS and ΔH report in insert of Fig. 3 are consistent with the values usually report in the literature for semi-crystalline polymers [20]. We observe a linear relationship between activation enthalpy and activation entropy associated with compensation phenomenon [20]. The corresponding relaxation times obey a compensation law:

$$\tau = \tau_c \exp\left\{\frac{\Delta H}{R}(T^{-1} - T_c^{-1})\right\} \quad (4)$$

where R is the universal gas constant, τ_c is the compensation time and T_c is the compensation temperature. For the α mode, $\tau_c = 3.10^{-2}$ s and $T_c = 84^\circ\text{C}$ i.e. $T_g + 25^\circ\text{C}$. Such a compensation phenomenon is characteristic of the distribution of relaxation times associated with the dielectric manifestation of glass transition.

Fig. 4 represents the activation enthalpy (ΔH) versus temperature for the β and α modes. The ΔH variation corresponding to a null activation entropy (also noted “Starkweather line” [21]) is symbolized by the dashed line. The enthalpies of the β relaxation are practically described by the “Starkweather line”. Contrarily, activation enthalpies associated with the α relaxation depart from the “Starkweather line”. It ascertains the localized behaviour of the β relaxation mode and the delocalised mobility of the α mode. The temperature range, the amplitude of the depolarization current and the cooperativity of this relaxation mode allow us to associate this relaxation with the dielectric manifestation of the glass transition of PA 6,9.

3.1.3. Dielectric relaxation map

The relaxation times extracted from the dissipative part of the dielectric permittivity by DDS are plotted on the Arrhenius diagram

Table 1
Activation energies and relaxation times of γ , β_1 , β_2 relaxation modes of PA 6,9.

Relaxation mode	Ea (kJ/mol)	τ_0 (s)
γ	31	2.5×10^{-13}
β_2	58	1×10^{-16}
β_1	99	2×10^{-22}

Table 2
VFT parameters and strength index $D = 1/(\alpha_{VTF} T_0)$ of α and α' modes of PA 6,9.

Relaxation mode	τ_0 (s)	T_0 (K)	α_{VTF} (K^{-1})	D
α	1×10^{-10}	293	1.6×10^{-3}	2.1
α'	4×10^{-10}	239	4.45×10^{-4}	9.4

of Fig. 5. The relaxation times of β and α modes extracted from fractional TSC measurements are also reported on Fig. 5. The three sub-vitreous dielectric relaxations have Arrhenius behaviour. The pre-exponential factors and the activation energies associated with these modes are reported in Table 1.

The low activation energy values related to these modes confirm their assignment to a localized mobility. This assumption is in good agreement with TSC data. By extrapolation, a “merging” between the sub-vitreous modes and α mode in the high frequency range can be expected. The α and α' modes exhibit a Vogel–Fulcher–Tammann (VFT) behaviour as for polyamide 11 [22–24]:

$$\tau = \tau_0 \exp \left\{ \frac{1}{\alpha_{VTF}(T - T_0)} \right\} \quad (5)$$

the VFT parameters of each mode are reported in Table 2.

The VFT parameters of α and α' modes are equivalent to VFT parameters measured on PA 11. The strength index $D = 1/\alpha_{VTF} T_0$, generally used as a quantitative measure of fragility, of the α' mode is higher than for α mode. It denotes that α' mode has a more strong behaviour according to Angell [22–24]. It is consistent with the fact that a constrained amorphous phase has a higher density of hydrogen bonds than a free amorphous phase.

The molecular mobility of dipolar entities in the amorphous phase of PA 6,9 has a similar behaviour than odd polyamide. According to these observations and to the chemical structure of PA 6,9 we might expect a piezoelectric activity.

3.2. Ferroelectric behaviour

Prior to polarization process, polyamide 6,9 films were cold-drawn to a ratio 3:1. The resulting stretched films were about 50 μm thick. Then, a high electric field was applied to polarize the PA 6,9 films. The variation of the electrical field versus time has a triangular shape.

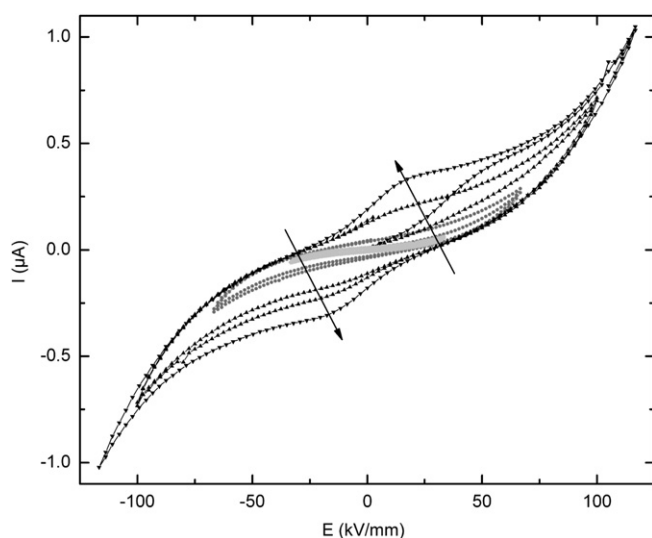


Fig. 6. Hysteresis cycle for PA 6,9 during polarization process for 4 successive cycles (1 ■, 2 ●, 3 ▲, 4 ▼). Arrows indicate the increase of PA 6,9 ferroelectric behaviour at each cycle.

During the polarization process, the current is measured versus applied field and it is reported on Fig. 6. The measured current increases with the applied electric field. The non linear behaviour of $I(E)$ is observed. For a poling field of 100 kV/mm, a shoulder appears at 25 kV/mm. The amplitude of the shoulder increases with the electric field. For an applied electric field up to 100 kV/mm, the shape of $I(E)$ curve is characteristic of a ferroelectric behaviour. The maximum electric field that could be applied on the PA 6,9 sample is 125 kV/mm. For upper electric field voltage, a breakdown is observed. As the amplitude of the shoulder increases up to an electric field of 125 kV/mm, we assume that the sample is not fully polarized.

Prior to pyroelectric and piezoelectric measurements, the sample was heated up to 120 °C in order to suppress thermo stimulated currents. The pyroelectric coefficient measured at room temperature is $p_{33} = -0.13 \mu\text{C}/\text{K}/\text{m}^2$. The piezoelectric coefficient recorded in the poling direction is $d_{33} = -0.25 \text{ pC}/\text{N}$. The ferroelectric activity of PA 6,9 is lower than the ferroelectric behaviour of PA 11 [18,21,22]. The piezoelectric activity of the PA 6,9 is demonstrated and it is consistent with conclusions from structural studies of PA 6,9 [10] but also of odd polyamides [25]. The low electroactive activity reported in this study has been attributed to the non saturated poling state of the sample.

4. Conclusion

Dielectric and electroactive properties of an even–odd polyamide, PA 6,9 are reported. Dielectric dynamic relaxation in a frequency range from 10^{-1} Hz – 10^6 Hz shows qualitative analogy with polyamides. For γ and β secondary relaxation modes, the analogy of the chemical structures is responsible for analogous behaviour. For the α primary relaxation mode, the density of hydrogen bonds sounds to play a key role: for a number of methylene groups lower than 6 i.e. PA 6,6, a strong behaviour is observed; when the number of methylene groups is higher i.e. PA 6,9 or PA 11, a fragile behaviour is found.

Up to now, only odd polyamides have been found to exhibit ferroelectric activity. For the first time, a ferroelectric activity has been pointed out in polyamide 6,9 after polarization up to 100 kV/mm and before voltage breakdown that appears for 125 kV/mm poling field. The weak piezo/pyro coefficients could be explained by a non saturated poling state PA 6,9. Such even–odd polyamides might be interesting for electroactive applications.

References

- [1] Kawai H. Japanese Journal of Applied Physics 1969;8:975.
- [2] Lovinger AJ. Science 1983;220:1115.
- [3] Oshiki M, Fukada E. Journal of Materials Science 1975;10:1.
- [4] Ibos L, Bernes A, Lacabanne C. Ferroelectrics 2005;320:48.
- [5] Samara GA, Bauer F. Ferroelectrics 1992;135:385.
- [6] Wang H, Zhang QM, Cross E, Sykes AO. Journal of Applied Physics 1994;74:3394.
- [7] Klein RJ, Runt J, Zhang QM. Macromolecules 2003;36:7220.
- [8] Bao HM, Song JF, Zhang J, Shen QD, Yang CZ, Zhang QM. Macromolecules 2007;40:2371.
- [9] Scheinbeim JL, Lee JW, Newman BA. Macromolecules 1992;25:3729.
- [10] Franco L, Cooper SJ, Atkins EDT, Hill MJ, Jones NA. Journal of Polymer Science 1998;36:1153.
- [11] Cui X, Yan D. European Polymer Journal 2005;41:863.
- [12] Sender C, Dantras E, Dantras – Laffont L, Lacoste MH, Dandurand J, Mauzac M, et al. Journal of Biomedical Materials Research Part B-Applied Biomaterials 2007;83B:628.
- [13] Havriliak S, Negami S. Journal of Polymer Science Part C 1966;14:99.
- [14] Kremer F, Schönhal A. Broad band dielectric spectroscopy. Berlin: Springer; 2003.
- [15] McCrum NG, Read BE, Williams G. Anelastic and dielectric effects in polymeric solids. New-York: John Wiley & Sons; 1967.
- [16] Prevorsek DC, Butler RH, Reimschuessel HK. Journal of Polymer Science Part A-2 1971;9:867.
- [17] Frank B, Frubinc P, Pissis P. Journal of Polymer Science, Part B: Polymer Physics 1996;34:1853.

- [18] Ibos L, Maraval C, Bernes A, Teyssedre G, Lacabanne C, Wu SL, et al. *Journal of Polymer Science, Part B: Polymer Physics* 1999;37:715.
- [19] Laredo E, Grimau M, Sanchez F, Bello A. *Macromolecules* 2003;36:9840.
- [20] Lacabanne C, Lamure A, Teyssère G, Bernès A, Mourgues M. *Journal of Non Crystalline Solids* 1994;884:172.
- [21] Starkweather HW. *Macromolecules* 1981;14:1277.
- [22] Ibos L. PhD thesis: University of Toulouse/F; 2000.
- [23] Angell CA. *Journal of Non Crystalline Solids* 1991;13:131.
- [24] Mei BZ, Scheinbeim JI, Newman BA. *Ferroelectrics* 1993;144:141.
- [25] Puggali J, Franco L, Aleman C, Subirana JA. *Macromolecules* 1998;31:8540.